Chellini *et al.*
Cellular & Molecular Biology Letters (2025) 30:63
https://doi.org/10.1186/s11658-025-00736-4

Cellular & Molecular Biology Letters

RESEARCH ARTICLE Open Access

YAP1 promoter-associated noncoding RNA affects Ewing sarcoma cell tumorigenicity by regulating YAP1 expression

Lidia Chellini[1*], Arianna Del Verme[1], Veronica Riccioni[1] and Maria Paola Paronetto[1,2*]

*Correspondence:

[1] Laboratory of Cellular and Molecular Neurobiology, IRCCS Santa Lucia Foundation, Rome, Italy
[2] Department of Movement, Human and Health Sciences, University of Rome "Foro Italico", Rome, Italy

Abstract

Background: Ewing sarcomas (ESs) are aggressive paediatric tumours of bone and soft tissues afflicting children and adolescents. Despite current therapies having improved the 5-year survival rate to 70% in patients with localized disease, 25% of patients relapse and most have metastasis at diagnosis. Resistance to chemotherapy, together with the high propensity to metastasize, remain the main causes of treatment failure. Thus, identifying novel targets for alternative therapeutic approaches is urgently needed.

Methods: Biochemical and functional analyses were carried out to elucidate the mechanism of regulation of YAP1 expression by *pncRNA_YAP1-1* in ES cells.

Results: Here, we identified a novel promoter-associated noncoding RNA, *pncRNA_YAP1-1*, transcribed from the *YAP1* promoter in ES cells. We found that *pncRNA_YAP1-1* level exerts antitumour effects on ES by destabilizing YAP1 protein. The molecular mechanism relies on the interaction of *pncRNA_YAP1-1* with the RNA binding protein FUS, which stabilizes the transcript. Furthermore, *pncRNA_YAP1-1* binding to TEAD impairs its interaction with YAP1, thus determining YAP1 translocation into the cytoplasm, its phosphorylation and degradation.

Conclusions: Overall, our findings reveal a novel layer of regulation of YAP1 protein expression by *pncRNA_YAP1-1* in Ewing sarcoma. Considering the role of YAP1 in therapy response and cell propensity to metastasize, our results indicate *pncRNA_YAP1-1* as an actionable target that could be exploited to enhance chemotherapy efficacy in Ewing sarcoma.

Significance: *PncRNA_YAP1-1* counteracts the YAP1 oncogenic transcriptional program in Ewing sarcoma cells by interfering with YAP1-TEAD interaction and impairing YAP1 protein stability. These findings uncover a novel treatment option for Ewing sarcoma.

Keywords: Promoter-associated noncoding RNA, YAP1, Ewing sarcoma, FUS

Graphical abstract

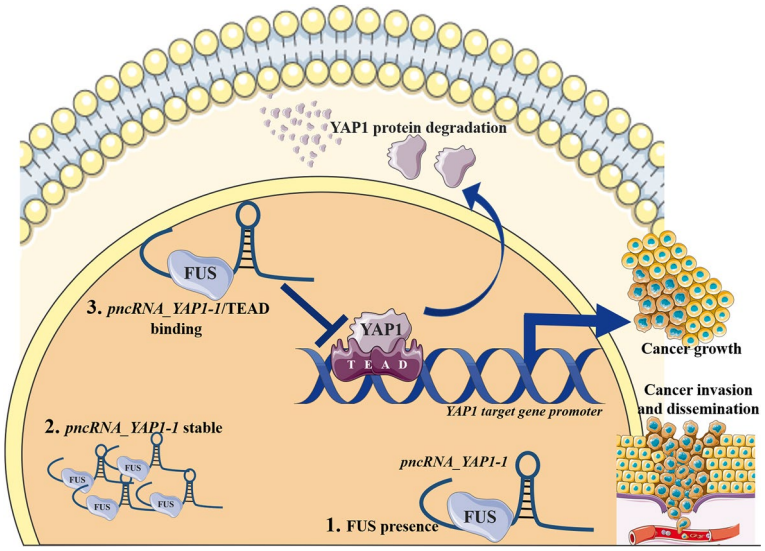

Introduction

Ewing sarcoma (ES) is the second most common bone cancer in adolescents and young adults, being highly aggressive and metastatic [1, 2]. The standard strategy to treat ES includes a multimodal approach consisting of chemotherapy, surgery and radiation [3]. Despite current therapies having improved the 5-year survival rate to 70% in patients with localized disease, 25% of patients relapse and most have metastasis at diagnosis [1, 4]. For these reasons, a deep understanding of the molecular mechanisms underlying ES initiation, progression and spreading is instrumental for identification of new players involved in the therapy response and in the metastasization process, thus contributing to novel targeted therapies.

The pivotal role of long noncoding RNAs (lncRNAs) in carcinogenesis is well documented in several cancers, including ES [5, 6]. Their participation in gene expression regulation occurs at transcriptional, epigenetic and post-transcriptional levels [5, 7–9]. Altered expression and function of lncRNAs have been implicated in several processes typically deregulated in cancer, including cell proliferation, growth and invasion, making them not only relevant biomarkers with prognostic significance but also potential therapeutic targets for cancer metastasis and drug resistance [9–12]. Numerous cellular signalling pathways are involved in the development and progression of ES, including the Hippo pathway, whose deregulation has also been observed in other tumours [13–15]. The transcriptional coactivator *Yes-associated protein 1* (YAP1), a critical member of the Hippo pathway, plays a key role in ES pathogenesis, representing a prominent target able to support cell proliferation, anchorage-independent growth and tumour progression [16, 17]. YAP/TAZ- regulated transcription of genes involved in tumour growth and metastasis has been found to correlate with the activity of EWS-FLI1, which is a crucial regulator in ES [18, 19].

Recent studies have highlighted the role of ncRNAs in the regulation of YAP/*transcriptional coactivator with PDZ-binding motif* (TAZ) signalling [20, 21]. LncRNAs can function as miRNA sponges, influencing the expression of different Hippo pathway effectors [22–26] or affecting protein-DNA/RNA/chromatin interactions to control YAP/TAZ signalling cascade [27] or even regulating *YAP1* mRNA stability [28]. Circular RNAs (*circRNAs*) mainly act as competing endogenous RNAs (ceRNAs) by sponging miRNAs, thus impacting the expression of different Hippo pathway components [29–32]. Furthermore, microRNAs (miRNAs) directly target YAP/TAZ mRNA [33–40], regulate the stability and nuclear translocation of the YAP/TAZ proteins [41, 42] or target other critical components of the Hippo pathway [43–45].

To date, only a small fraction of lncRNAs have been functionally characterized in ES [5, 7, 46], and no indication about the role of lncRNAs influencing YAP1 expression in this tumour are available yet. Among the noncoding transcripts, promoter-associated noncoding RNAs (pncRNAs) are transcribed from the promoter region proximal to the transcription start-sites (TSS) of protein-coding or non-coding genes, canonically operating as cis-acting elements to regulate their host gene [47, 48]. In this study, we investigate the function of a not yet characterized *YAP1* promoter-associated ncRNA (*pncRNA_YAP1-1*) in ES cells. We found that enhanced *pncRNA_YAP1-1* level exerts antitumour effects on ES cells, through destabilization of YAP1 protein. Our findings explore an additional layer of regulation of YAP1 protein expression by *pncRNA_YAP1-1* in ES cells. Since YAP1 abundance affects therapy response and cell propensity to metastasize [13, 49], our results suggest that modulation of *pncRNA_YAP1-1* levels could represent a novel therapeutic strategy to target ES.

Materials and methods

Cell culture, treatments and transfection

Different ES cell lines were obtained from DSMZ: TC-71 (cat no. ACC516), SK-ES1 (cat. no. ACC518), RD-ES (cat. no. ACC260) and SK-N-MC (cat. no. ACC203). TC-71 and SK-N-MC cell lines were maintained in Iscove's modified Dulbecco's medium (IMDM, GIBCO), SK-ES1 cell lines were maintained in McCoy's 5a medium (Gibco) and RD-ES cell lines were maintained in RPMI-1640 (Gibco). All media were supplemented with 10% fetal bovine serum (FBS) (Gibco), 50 units/mL penicillin and 50 mg/mL streptomycin. Cells were incubated at 37 °C in a humidified atmosphere with 5% CO_2. All cells were tested routinely for *Mycoplasma* contamination (N-GARDE *Mycoplasma* PCR Reagent set, Euroclone, cat. no. EMK090020). For serum deprivation experiments, cells were grown in serum-free media for 24 h and collected, together with the control sample (complete media). When necessary, cells were treated with: cycloheximide (CHX) (12.5 µg/mL, Selleckchem cat. no. S7418) for 4 h; MG-132 (25 µM, Selleckchem cat. no. S2619) or dimethyl sulfoxide (DMSO) for 3.5 h; BEZ-235 (300 nM, Selleckchem cat. no. S1009) or DMSO for 16 h; RAD-001(25 nM, Selleckchem cat. no. S1120) or DMSO for 16 h; OLAPARIB (300 nM, Selleckchem cat. no. S1060) or DMSO for 24 h; ETOPOSIDE (5 µM, Selleckchem cat. no. S1225) or DMSO for 24 h.

Cells were transfected using Lipofectamine 2000 (Thermo Fisher Scientific) according to the manufacturer's instructions. Cells were transfected for 48 h and then lysed. siRNA sequences are the following: siCTRL: 5′ GGC AGC AGA GUU CAC UGC

U-dCdG; si*YAP1*: (5′–3′) UUUGCUGGUAAUUGCGUGGAGGACC-dCdG; si*YAP1#2*: (5′–3′) GACCAAUAGCUCAGAUCCUUU-dCdG; si*PncRNA_YAP1-1#A*: (5'-3') UUU UCGCUGCAA GUUGCUACAUUCC [dC][dG]; si*PncRNA_YAP1-1#B*: (5′–3′) GCG AGGAUAGAUUGGAGU UAA [dC][dG]; si*FUS*: sc-40563. For ectopic expression of *pncRNA_YAP1-1*, cells were transiently transfected with the plasmid using Lipofectamine 2000 (Thermo Fisher Scientific) according to the manufacturer's instructions. Cells were transfected for 48 h and then lysed. The pcDNA3.1_pncYAP1-1 plasmid was obtained as described.

Plasmid construct

PncRNA_YAP1-1 sequence template was generated from SK-N-MC cDNA using the Phusion High-Fidelity DNA Polymerase (Thermo Fisher Scientific cat. no. F630S) and the primers Fw-Xho I and Rv-Not I. The amplified product was cloned into the XhoI and NotI sites of pcDNA3.1(-) vector to generate the pcDNA3.1_pncYAP1-1 plasmid. The ligase reaction was performed by using T4 DNA Ligase (Promega) following the manufacturer's instructions. The sequence of plasmid was confirmed by DNA sequence analysis (Eurofins, Italy). The sequences of all primers used are listed in Supplementary Table S1.

RNA isolation and reverse transcription-quantitative polymerase chain reaction (RT-qPCR)

Total RNA was extracted from cells by using TRIzol Reagent (Thermo Fisher Scientific) according to the manufacturer's instructions. RNA was subjected to DNAse digestion (Life Technologies, cat. no. AM2238), and the first-strand cDNA was obtained from 1 μg of RNA using M-MLV Reverse Transcriptase (Promega, Madison, WI, USA) following the manufacturer's instructions. cDNA was examined for quantitative-PCR using Takara Universal qPCR Master Mix (NEB, New England Biolabs, cat. no. M3003) on a Quant Studio 1 real-time PCR machine according to the manufacturer's instructions. Primers used for RT-qPCR analyses are listed in Supplementary Table S1. The levels of gene expression were determined by normalizing to *GAPDH* mRNA expression and expressed as relative mRNA level ($2^{-\Delta\Delta Ct}$).

Sub-cellular fractionation

For protein extraction, cellular pellets were re-suspended in hypotonic buffer RSB10 (10 mM Tris–HCl at pH 7.4, 10 mM NaCl, 2.5 mM $MgCl_2$, 1 mM DTT, protease inhibitor cocktail). After incubation on ice for 7 min, samples were centrifuged at 1000*g* for 7 min. Supernatant (cytosolic extract) was collected while pelleted nuclei were then resuspended in RSB100 (hypotonic buffer supplemented with 90 mM NaCl and 0.5% Triton X-100), sonicated and centrifuged at 10,000*g* for 15 min to obtain nuclear extract. Cytosolic and nuclear extracts were analysed by western blot.

For RNA extraction, cellular pellets were incubated for 10 min at 4 °C in cold extraction buffer (150 mM NaCl; 1.5 mM $MgCl_2$; 10 mM Tris–HCl; 1 mM DTT, 0.1% NP40) and centrifuged at 1500*g* for 5 min. Trizol was added to the pellet nuclei, and supernatant corresponding to the cytosolic fraction was transferred in a new tube and Trizol was added.

Fluorescent in situ hybridization (FISH)

FISH was performed by using Stellaris™ RNA FISH according to the manufacturer's instructions (LGC, Biosearch Technologies, cat. no. SMF-1063-5). Cells were grown in cover glass, washed with phosphate-buffered saline (PBS) and fixed with fixation buffer (3.7% formaldehyde in PBS) at room temperature for 10 min. Cells were washed twice with PBS and permeabilized in 70% ethanol for > 1 h at 4 °C. Finally, cells were incubated with Stellaris™ RNA FISH Wash Buffer A (LGC, Biosearch Technologies, cat. no. SMF-WA1-60) for 5 min at room temperature. Then, hybridization of the Custom Stellaris™ RNA FISH Probes designed against *pncRNA_YAP1_1* (125 nM) was carried out in the dark at 37 °C for 16 h in the Stellaris RNA FISH Hybridization Buffer (LGC, Biosearch Technologies, cat. no. SMF-HB1-10). Cells were incubated twice with Buffer A in the dark at 37 °C for 30 min. The second wash contained 4′,6-Diamidino-2-phenylindole, dihydrochloride (DAPI) for nuclear staining. Cells were washed with Stellaris™ RNA FISH Wash Buffer B in the dark at room temperature for 5 min and mounted and imaged using an Invitrogen EVOS M5000 microscope.

Custom Stellaris™ RNA FISH Probes were designed against *pncRNA_YAP1-1* by utilising the Stellaris RNA FISH Probe Designer (LGC, Biosearch Technologies, Petaluma, CA, USA) available online at www.biosearchtech.com/stellarisdesigner. The Custom Stellaris™ RNA FISH Probes against *pncRNA_YAP1-1* were labelled with Quasar 570 Dye (LGC, Biosearch Technologies).

Protein extraction and western blot (WB) analysis

For protein extraction, cells were washed with ice-cold phosphate-buffered saline (PBS), resuspended in lysis buffer (50 mM Tris-HCl pH 7.5, 350 mM NaCl, 1 mM $MgCl_2$, 0.5 mM EDTA, 0.1 mM EGTA), 1% Nonidet P-40, 10 mM B-glycerophosphate 100 mg/mL PMSF, 0.5 mM Na-orthovanadate, 10 mM sodium fluoride, Protease-Inhibitor Cocktail (Sigma-Aldrich) and kept on ice for 20 min. The supernatant, obtained by centrifugation at 12,000 rpm for 10 min, was used to determine protein concentrations by Bradford assay (Bio-Rad Laboratories, cat. no. 5000205). Cell lysates were resolved by SDS-PAGE and transferred to PVDF membranes (GE, Healthcare). The membranes were saturated in T-TBS (TBS with 0.1% Tween 20), containing 5% milk. Primary antibody incubations were performed in T-TBS with 5% BSA overnight at 4 °C. After washing, the membranes were incubated with the appropriate secondary peroxidase conjugated antibody for 1 h in T-TBS. The following antibodies were used for immunoblotting: mouse anti-GAPDH (Santa Cruz Biotechnology, cat. no. sc-365062, RRID:AB_10847862), mouse anti-YAP1 (Santa Cruz Biotechnology, cat. no. sc-101199, RRID:AB_1131430), rabbit anti-H3 (Novus, cat. no. NB500-171, RRID:AB_10001790), rabbit anti-TAZ (ABclonal-A8202, RRID:AB_2721146), mouse anti-FUS (sc-47711, RRID:AB_2105208), rabbit anti-P-YAP1 (Ser127) (GeneTex, GTX130424), mouse anti-CSTF2 (sc-166647, RRID:AB_2086367), mouse anti-TEAD (TEF-3 B-5, sc-390578). Proteins were visualized by chemiluminescence detection system (Clarity Western ECL Substrates, Bio-Rad Laboratories, cat. no. 1705061). Quantification analyses were performed using Image J Software (Image J, RRID:SCR_003070) (https://imagej.nih.gov/ij/).

MTS assay

To assess cell viability, 5×10^3 cells were plated in each well of a 96-culture plate. Subsequently, 48 and 72 h after transfection, the absorbance (O.D. 490 nm) was measured by using Cell Titer Aqueous Assay (Promega) with MTS tetrazolium following the manufacturer's instructions.

Invasion assay

The assays were carried out using 1×10^4 cells plated on an insert with 8.0-µm pore-sized membranes (Sarstedt, cat. no. 833932800), which were coated with laminin (10 µg/mL). Cells were left to invade for 12 h at 37 °C, and the invading cells were fixed with 70% ethanol at room temperature for 10 min. Then, membrane was stained with 0.2% crystal violet solution (Sigma-Aldrich) for 7 min. Membranes were dipped into distilled water to remove the excess of crystal violet and allowed to dry. Each experiment was repeated three times. From each transwell, four images were taken at 10X magnification by an Invitrogen EVOS M5000 microscope, and quantification of the individual photos was performed using Image J Software (Image J, RRID:SCR_003070).

Wound healing assay

Transfected cells were plated on six-well plates and grown until confluence. After 24 h, using a sterile 200-µl tip, a single scratch was made through the middle of each well. Photographs of wound closing were taken at time 0 (T0, 24 h from transfection) and at the end of the experiment (T1, 48 h from transfection), with an Invitrogen EVOS M5000 microscope. Images were analysed with Image J Software (Image J, RRID:SCR_003070).

In vitro RNA transcription

Linear DNA template for the in vitro RNA synthesis was obtained using PCR products using forward primer containing the T7 promoter sequence and reverse primers at the 3′ end of *pncRNA_YAP1-1*. Amplified bands were gel-purified and used as templates (1 µg) for in vitro RNA transcription with T7 polymerase (MEGAscript™ T7 Transcription Kit, Life Technologies, cat. no. AM1334) of the *pncRNA_YAP1-1*, then purified by G25 Sephadex columns (GE Healthcare) and diluted in RNAse-free water (Sigma-Aldrich).

Biotin-RNA pull-down

Biotin-RNA pull-down was performed as previously described [50, 51], with minor changes. SK-N-MC nuclear extracts were precleared for 60 min on Sepharose beads in the presence of 0.25 mg/mL yeast tRNA to reduce non-specific RNA–protein interactions. Precleared extracts were incubated with Streptavidin-Sepharose beads pre-incubated for 1 h with 0.05% bovine serum albumin (BSA) and the biotinylated *pncRNA_YAP1-1* oligonucleotides to be tested. Incubation was carried out for 45 min at 30 °C, under rotation. After stringent washes, beads were washed three times with lysis buffer (150 mM NaCl, 50 mM Tris–HCl at pH 8.0, 1% NP-40) and then eluted in Laemmli buffer 1X. Samples were analysed by western blot as previously described.

Immunoprecipitation (IP)

Cell protein extracts (see the paragraph "Protein extraction") (500 µg) were precleared and then incubated with Dynabeads conjugated with Protein G (Thermo Fisher Scientific cat. no. 10003D) and 1 µg of mouse anti-YAP1 (sc-101199), mouse anti-TEAD (sc-390578) or purified mouse IgGs (Thermo Fisher Scientific) overnight at 4 °C, under constant rotation. After three washes with lysis buffer, beads were eluted in Laemmli buffer. Isolated complexes were analysed by western blot.

Statistical analysis

Statistical analysis was conducted using GraphPad Prism software and the values represent mean ± standard deviation (SD) obtained from three independent experiments. The statistical significance of the differences was determined using student's *t* test (to compare two conditions) or analysis of variance (ANOVA) test (to compare more than two conditions). Statistical significance was defined as: $^{*}p < 0.05$; $^{**}p < 0.01$; $^{***}p < 0.001$; $^{****}p < 0.0001$.

Results

AP0015271.1 and AP0015271.2 are *YAP1*-promoter associated non-coding RNAs

Given the relevance of YAP1 in controlling tumour progression and metastasis [13, 15, 52], we investigated its possible regulation by *cis* regulatory transcript transcribed from its own promoter. To this aim, we queried the UCSC Genome Browser (https://genome.ucsc.edu/) for transcribed sequences upstream of the *YAP1* start site. We found two not yet characterized lncRNAs, associated with the *YAP1* promoter, annotated as AP001527.2 (ENST00000614441.1) and AP001527.1 (ENST00000566440.1) (Fig. 1A), which is renamed in this manuscript as *pncRNA_YAP1-1* and *pncRNA_YAP1-2*, respectively. The putative *pncRNA_YAP1-1* is located on the human chromosome 11,

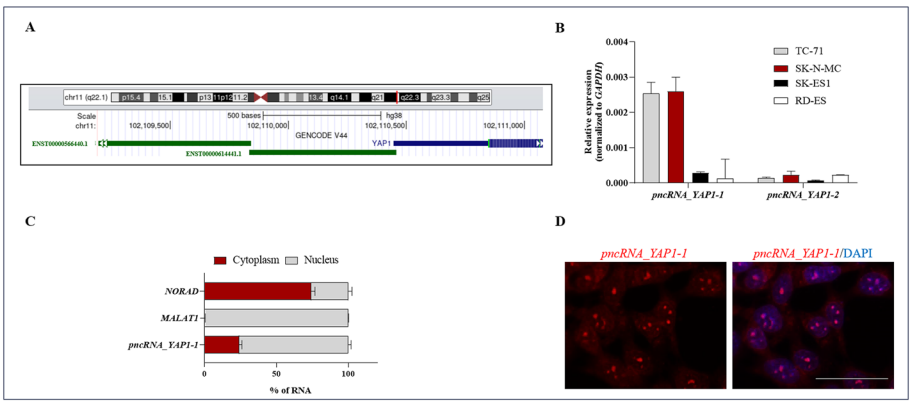

Fig. 1 *pncRNA_YAP1-1* and *pncRNA_YAP1-2* are associated with *YAP1* promoter. **A** Schematic representation of *YAP1* locus gene from the Genome Browser, where *pncRNAs_YAP1* are annotated (green box). ENST00000614441.1 (AP0015271.2) is *pncRNA_YAP1-1* and ENST00000566440.1 (AP0015271.1) is *pncRNA_YAP1-2*. **B** Endogenous *pncRNA_YAP1-1* and *pncRNA_YAP1-2* levels were analysed in different ES cell lines. **C** Cytosolic and nuclear RNA was extracted from SK-N-MC cells and analysed by RT-qPCR. *MALAT1* is used as nuclear marker and *NORAD* as cytosolic marker. Values are the mean ± SD of three independent experiments, expressed as % of total RNA. **D** FISH experiment was performed by using Stellaris™ RNA FISH. Fixed SK-N-MC cells were probed for *pncRNA_YAP1-1* (probes labelled with Quasar 570, red) and DAPI (nuclear staining) and imaged with 40X objective. Scale bar: 75 µm

displaying the 102 109 827-102 110 457 (*hg38*) coordinates. This antisense lncRNA is formed by a single exon of 631 nucleotides. The putative *pncRNA_YAP1-2* is located on the human chromosome 11, at the genomic locus 102 107 886-102 109 842 (*hg38*). *PncRNA_YAP1-2* is a sense lncRNA formed by a single exon of 1957 nucleotide. We first assessed the abundance of *pncRNA_YAP1-1* and *pncRNA_YAP1-2* by RT-qPCR in four different ES cell lines. Our results show that *pncRNA_YAP1-1* is expressed predominantly in TC-71 and SK-N-MC cells, while the expression levels in the SK-ES1 and RD-ES cells are reduced (Fig. 1B). Moreover, we found that *pncRNA_YAP1-2* is only barely detectable in all the ES cell lines tested. Given this result, we decided to focus on the *pncRNA_YAP1-1*. Further investigation using the Coding Potential Calculator (http://cpc2.gao-lab.org) revealed that *pncRNA_YAP1-1* has no protein-coding potential (Supplementary Fig. 1A). In addition, biochemical subcellular fractionation experiments showed that *pncRNA_YAP1-1* is predominantly localized in the nucleus of SK-N-MC and TC-71 cells (Fig. 1C and Supplementary Fig. 1B). Furthermore, by analysing the GSE150722 dataset of patients with ES [53], we found that *pncRNA_YAP1-1* is expressed in ES tumour samples at higher or comparable levels than other noncoding RNAs, such as *MALAT1* and *HULC* (Supplementary Fig. 1C). RNA FISH experiments with fluorescent probes targeting *pncRNA_YAP1_1* (see Methods section for the experimental details) confirmed the biochemical results (Fig. 1D). In parallel, we analysed the expression level of the neighbouring *YAP1* gene. We found that YAP1 expression is higher in TC-71 and SK-N-MC cells at both mRNA and protein level (Fig. 2A, B) in comparison with the SK-ES1 and RD-ES cells.

The involvement of YAP1 in ES pathogenesis was extensively documented by several laboratories [16–19, 52]. YAP1 expression was associated with the presence of tumour progression and poor prognosis in patients with ES [17, 18, 20]. In line with these studies, our results demonstrate decreased cell proliferation (Fig. 2C–E and Supplementary Fig. 2A–C) and invasion (Fig. 2F and Supplementary Fig. 2D) after reduction of YAP1 expression in SK-N-MC cells, paralleling the downregulation of YAP1 target genes (Fig. 2G and Supplementary Fig. 2E).

Collectively, these findings suggest that targeting YAP1 expression could be exploited to limit ES invasiveness.

PncRNA_YAP1-1 impacts ES cell proliferation and invasion by decreasing YAP1 protein

Since YAP1 displays higher expression in SK-N-MC and TC-71 cells, established in patients with metastasis, than in RD-ES and SK-ES1 cells, derived from primary tumours, we hypothesized that the expression of *YAP1* could contribute to sustaining the invasive and aggressive phenotype of ES.

To assess the possible involvement of *pncRNA_YAP1-1* on the control of YAP1 expression and ES cell growth, the full-length sequence of *pncRNA_YAP1-1* was cloned into a pcDNA3.1 vector (pcDNA3.1_pncYAP1-1) for transient expression in ES cells. Upregulation of *pncRNA_YAP1-1* after transfection of pcDNA3.1_pncYAP1-1 was confirmed by RT-qPCR (Fig. 3A, Supplementary Fig. 3A). Remarkably, we found that *pncRNA_YAP1-1* overexpression was sufficient to reduce the proliferative capacity of SK-N-MC and TC-71 cells (Fig. 3B, Supplementary Fig. 3B). Moreover, the wound healing assay showed that *pncRNA_YAP1-1* overexpression resulted in a slower ES cell migration

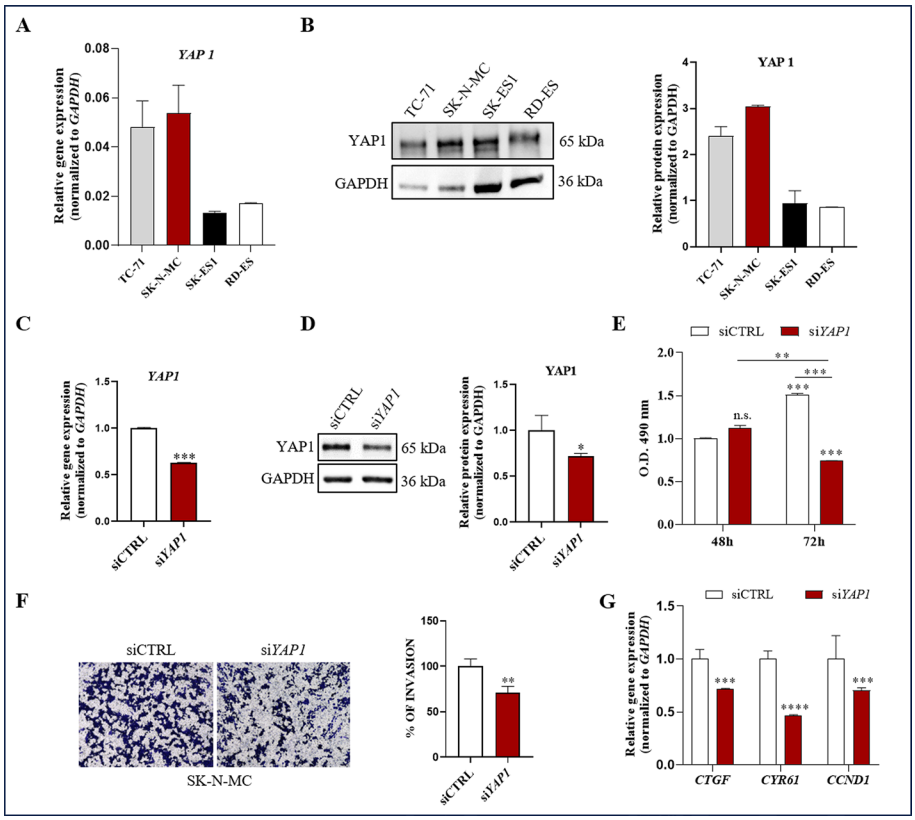

Fig. 2 YAP1 contributes to Ewing sarcoma tumour growth. Endogenous *YAP1* mRNA (**A**) and protein (**B**) level were analysed in different ES cell lines by RT-qPCR and immunoblot (IB) analysis, respectively. GAPDH was used as control. SK-N-MC cells were transfected with a control siRNA (siCTRL) or a siRNA specific for *YAP1* (si*YAP1*) and YAP1 expression was analysed by RT-qPCR (**C**) and WB analysis (**D**). Histograms represent the mean ± SD of three independent experiments, considering the siCTRL as 1. **E** SK-N-MC cells were transfected as in **C** and analysed by MTS assay after 48 and 72 h. Values are the mean ± SD of three independent experiments, considering the siCTRL at 48 h as 1. **F** SK-N-MC cells were transfected as in **C** and invasion assay was performed. The crystal violet-stained invading cells were photographed (left) and counted (right). Values are the mean ± SD of three independent experiments, considering the invasion of siCTRL sample as 100%. **G** SK-N-MC cells were transfected as in **C** and the mRNA level of YAP1 target genes was analysed by RT-qPCR. Values are the mean ± SD of three independent experiments. Statistical analyses in **C**, **D**, **F**, and **G** were performed using Student's *t*-test, and in **E**, analyses were performed by *two-way* ANOVA, *p*-values: *$p \leq 0.05$; **$p \leq 0.01$; ***$p \leq 0.001$; ****$p \leq 0.0001$

rate compared with the control group (Fig. 3C, Supplementary Fig. 3C). In addition, *pncRNA_YAP1-1* overexpression reduced cell invasion, as documented by transwell invasion assays (Fig. 3D, Supplementary Fig. 3D). Taken together, these results indicate that *pncRNA_YAP1-1* overexpression reduces ES cell proliferation and invasion.

Next, we explored the effect of modulation of *pncRNA_YAP1-1* on YAP1 expression. RT-qPCR analyses showed that *YAP1* mRNA expression was not affected by the increase of *pncRNA_YAP1-1* induced by overexpression, both in SK-N-MC and in TC-71 cells (Fig. 3E, Supplementary Fig. 3E). Instead, YAP1 protein was reduced after *pncRNA_YAP1-1* overexpression (Fig. 3F, Supplementary Fig. 3F). Accordingly, reduced YAP1 protein level, induced by *pncRNA_YAP1-1* overexpression, correlated with reduced expression of YAP1 target genes, such as *CTGF* (connective tissue growth factor),

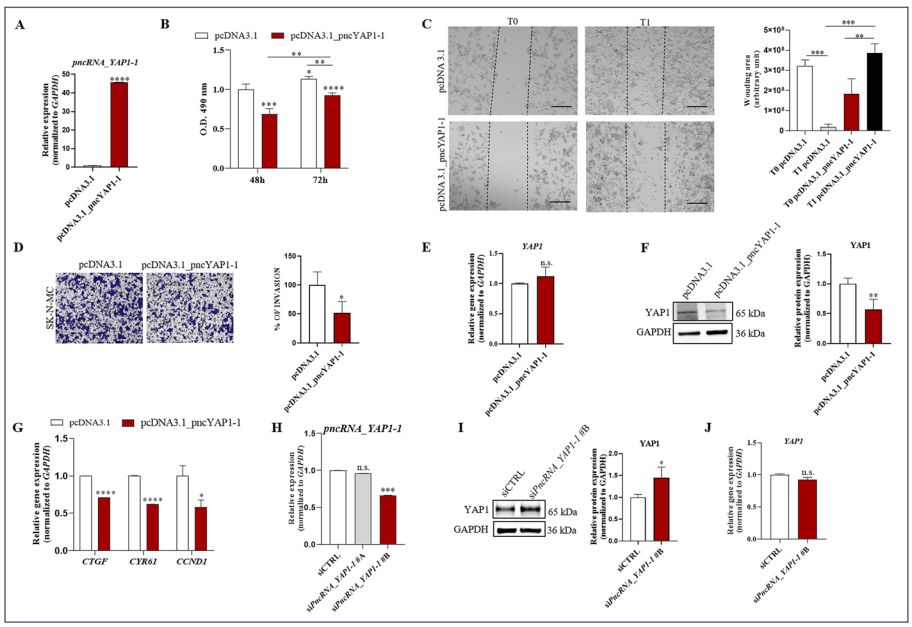

Fig. 3 *pncRNA_YAP1-1* overexpression reduces YAP1 protein level and attenuates the tumorigenic phenotype of ES cells. **A** SK-N-MC cells were transfected with empty vector (pcDNA3.1) or a plasmid overexpressing *pncRNA_YAP1-1* (pcDNA3.1_pncYAP1-1), and *pncRNA_YAP1-1* expression was analysed by RT-qPCR. Histograms represent the mean ± SD of three independent experiments, considering the pcDNA3.1 as 1. **B** SK-N-MC cells were transfected as in **A** and analysed by MTS assay after 48 and 72 h. Values are the mean ± SD of three independent experiments, considering the pcDNA3.1 at 48 h as 1. **C** SK-N-MC cells were transfected as in **A** and wound healing assay was performed. Cells were photographed, and the wounding area was measured. Values are the mean ± SD of three independent experiments. Magnification: 10X. **D** SK-N-MC cells were transfected as in **A**, and invasion assay was performed. The crystal violet-stained invading cells were photographed (left) and counted (right). Values are the mean ± SD of three independent experiments, considering the invasion of pcDNA3.1 sample as 100%. SK-N-MC cells were transfected as in **A**, and YAP1 expression was analysed by RT-qPCR (**E**) and WB analysis (**F**). Histograms represent the mean ± SD of three independent experiments, considering the pcDNA3.1 as 1. **G** SK-N-MC cells were transfected as in **A**, and the mRNA level of YAP1 target genes was analysed by RT-qPCR. **H** SK-N-MC cells were transfected with a control siRNA (siCTRL) or a siRNA specific for *pncRNA_YAP1-1* (si*PncRNA_YAP1-1#A* or si*PncRNA_YAP1-1#B*), and *pncRNA_YAP1-1* expression was evaluated by RT-qPCR. SK-N-MC cells were transfected with a control siRNA (siCTRL) or a siRNA specific for *pncRNA_YAP1-1* (si*PncRNA_YAP1-1 #B*), and YAP1 expression was analysed by WB analysis (**I**) and RT-qPCR (**J**). Histograms represent the mean ± SD of three independent experiments, considering the siCTRL as 1. Statistical analyses in **A**, **D**–**J** were performed using Student's *t*-test, in **B** and **C**, analyses were performed by *two-way* ANOVA, *p*-values: *$p \leq 0.05$; **$p \leq 0.01$; ***$p \leq 0.001$; ****$p \leq 0.0001$

CYR61 (CYsteine-Rich angiogenic inducer 61) and *CCND1* (Cyclin D1), both in SK-N-MC and in TC-71 cells (Fig. 3G, Supplementary Fig. 3G).

To understand the effective role of *pncRNA_YAP1-1*, we knocked down its expression by using two different siRNAs, with the second one, named "B" (Fig. 3H, Supplementary Fig. 4A), which is more efficient in downregulating *pncRNA_YAP1-1* transcript. Notably, *pncRNA_YAP1-1* downregulation correlated with the increase of YAP1 protein level (Fig. 3I, Supplementary Fig. 4B), without affecting *YAP1* transcript (Fig. 3J, Supplementary Fig. 4C).

Collectively, these results suggest that *pncRNA_YAP1-1* could have an impact on ES growth by reducing YAP1 abundance and, accordingly, YAP1 transcriptional activity.

YAP1 protein stability is affected by *pncRNA_YAP1-1*

YAP1 protein exerts its oncogenic functions through the transcriptional activation of target genes in the cell nucleus. Moreover, post-translational modifications of YAP protein play crucial roles in regulating its stability, function and distribution [13, 54]. Since YAP1 protein level and activity decreased after *pncRNA_YAP1-1* overexpression, we decided to analyse YAP1 protein distribution. Subcellular

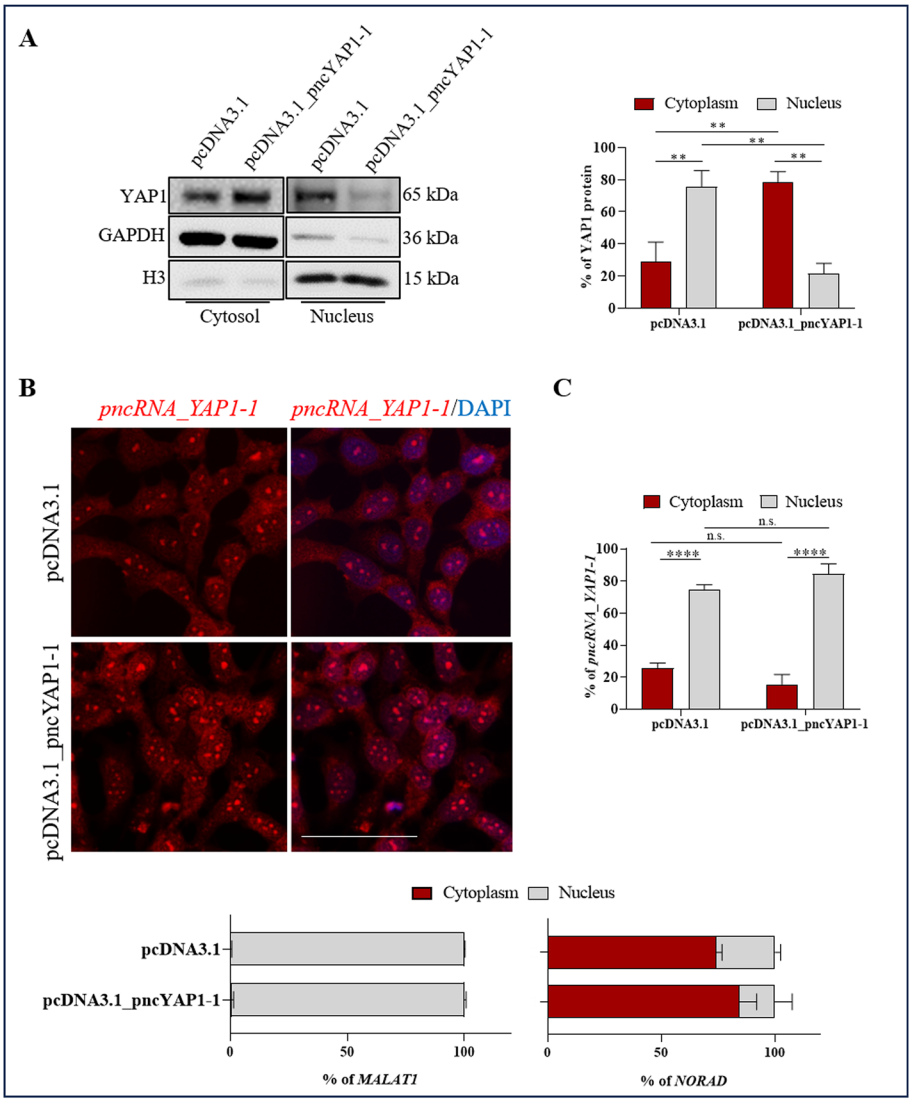

Fig. 4 *pncRNA_YAP1-1* overexpression promotes YAP1 cytoplasmic accumulation. **A** SK-N-MC cells were transfected with empty vector (pcDNA3.1) or a plasmid overexpressing *pncRNA_YAP1-1*, and cytosolic and nuclear protein extracts were obtained to monitor YAP1 localization. GAPDH was used as cytosolic marker, and H3 was used as nuclear marker. Histograms represent the mean ± SD of three independent experiments, expressed as %. **B** Cells were transfected as in **A** and fixed, and FISH experiment was performed by using Stellaris™ RNA FISH. Cells were probed for *pncRNA_YAP1-1* (probes labelled with Quasar 570, red) and DAPI (nuclear staining) and imaged with 40X objective. Scale bar: 75 µm. **C** Cytosolic and nuclear RNA was extracted from SK-N-MC cells transfected as in **A** and analysed by RT-qPCR. *MALAT1* is used as nuclear marker and *NORAD* as cytosolic marker. Values are the mean ± SD of three independent experiments, expressed as % of total RNA. Statistical analyses were performed using Student's *t*-test, *p*-values: $*p \leq 0.05$; $**p \leq 0.01$; $***p \leq 0.001$; $****p \leq 0.0001$

fractionation experiments revealed YAP1 cytoplasmic accumulation upon *pncRNA_YAP1-1* overexpression (Fig. 4A). Importantly, we did not observe any significant change in the localization of *pncRNA_YAP1-1*, which remained predominantly nuclear, despite its expression levels being significantly increased after overexpression (Fig. 4B, C). An increase of YAP1 protein in the nuclear fraction was observed after *pncRNA_YAP1-1* silencing (Supplementary Fig. 4D). Taken together, these results suggest that *pncRNA_YAP1-1* could participate in a post-transcriptional regulation of YAP1 expression.

Since *pncRNA_YAP1-1* upregulation significantly reduced the total protein level of YAP1, without affecting its mRNA level, we performed cycloheximide (CHX) chase assay to investigate whether *pncRNA_YAP1-1* could have an impact on YAP1 protein stability. We found that YAP1 protein was considerably reduced after 4 h of CHX treatment in SK-N-MC cells (Fig. 5A), and its half-life resulted decreased in *pncRNA_YAP1-1*-overexpressing cells (Fig. 5B). To further ascertain whether *pncRNA_YAP1-1* facilitates YAP1 protein degradation, we treated ES cells with the proteasome inhibitor MG-132. We found that MG-132 treatment was sufficient to prevent the reduction of YAP1 protein induced by ectopic expression of *pncRNA_YAP1-1* (Fig. 5C). In line with these results, we observed that the increase of YAP1 protein induced by *pncRNA_YAP1-1* silencing

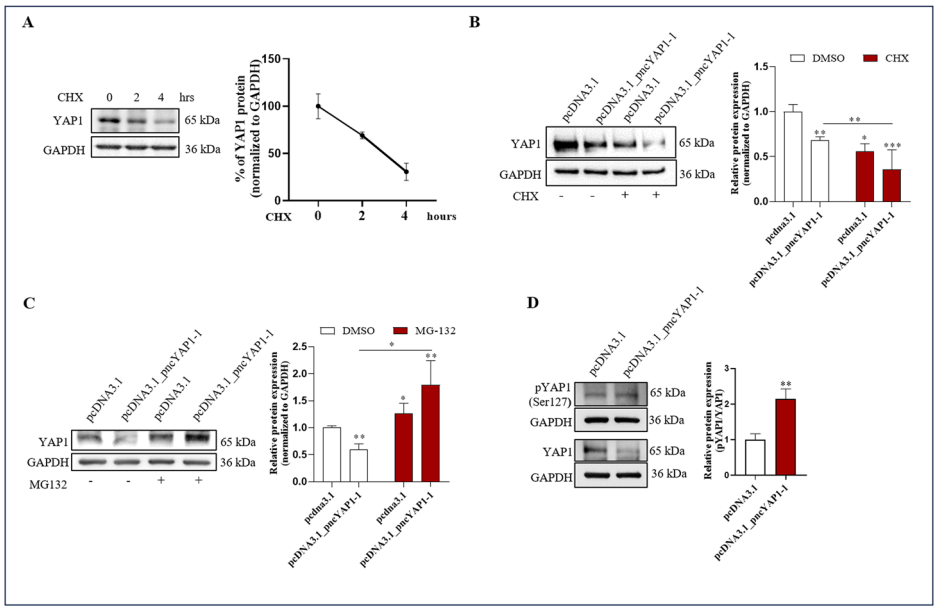

Fig. 5 *pncRNA_YAP1-1* overexpression affects YAP1 protein stability. **A** SK-N-MC cells were treated with CHX (12.5 µg/mL) for the indicated time, and YAP1 protein level was analysed. The graph represents the quantification of YAP1 protein after CHX treatment, expressed as %, considering the sample at time 0 as 100%. **B** SK-N-MC cells were transfected with empty vector (pcDNA3.1) or a plasmid overexpressing *pncRNA_YAP1-1* and were treated or not treated (DMSO) with CHX (12.5 µg/mL) for 4 h. Histograms represent the mean ± SD of three independent experiments, considering the sample DMSO pcDNA3.1 as 1. **C** SK-N-MC cells were transfected as in **B** and were treated or not treated (DMSO) with MG-132 (25 µM) for 3.5 h. Histograms represent the mean ± SD of three independent experiments, considering the sample DMSO pcDNA3.1 as 1. **D** SK-N-MC cells were transfected with empty vector (pcDNA3.1) or a plasmid overexpressing *pncRNA_YAP1-1* and P-YAP1 (Ser127) and total YAP1 protein level was analysed by western blot. Values are the mean of the ratio P-YAP1/YAP1 ± SD of three independent experiments, considering the sample pcDNA3.1 as 1. Statistical analyses were performed using Student's *t*-test, *p*-values: *$p \leq 0.05$; **$p \leq 0.01$; ***$p \leq 0.001$; ****$p \leq 0.0001$

was abolished by CHX treatment (Supplementary Fig. 4E). Conversely, MG-132 treatment enhanced the accumulation of YAP1 protein after *pncRNA_YAP1-1* silencing (Supplementary Fig. 4F).

Since YAP1 protein abundance is regulated by phosphorylation [13], we assessed the effect of *pncRNA_YAP1-1* expression on the phosphorylation of YAP1 (Ser127) protein. Interestingly, *pncRNA_YAP1-1* overexpression led to an increase in YAP1 phosphorylation (Fig. 5D), whereas *pncRNA_YAP1-1* silencing decreased YAP1 phosphorylation, thus contributing to YAP1 protein stabilization and upregulation (Supplementary Fig. 4G).

These results suggest that *pncRNA_YAP1-1* can affect cell tumorigenicity by promoting YAP1 cytoplasmic accumulation and YAP1 protein degradation in ES cells.

FUS is involved in the decrease of YAP1 protein induced by *pncRNA_YAP1-1*

LncRNAs can regulate gene expression by recruiting RNA binding proteins (RBPs) [6, 9]. To understand the molecular mechanism underlying *pncRNA_YAP1-1* regulation, we queried the online prediction tool "annolc" (https://annolnc.gao-lab.org/) to identify potential interactors of *pncRNA_YAP1-1* transcript. Cross-linking and immunoprecipitation sequencing (CLIP-seq) data showed that *pncRNA_YAP1-1* is bound by the Cleavage Stimulation Factor Subunit 2 (*CSTF2*) [55] and the RBP Fused

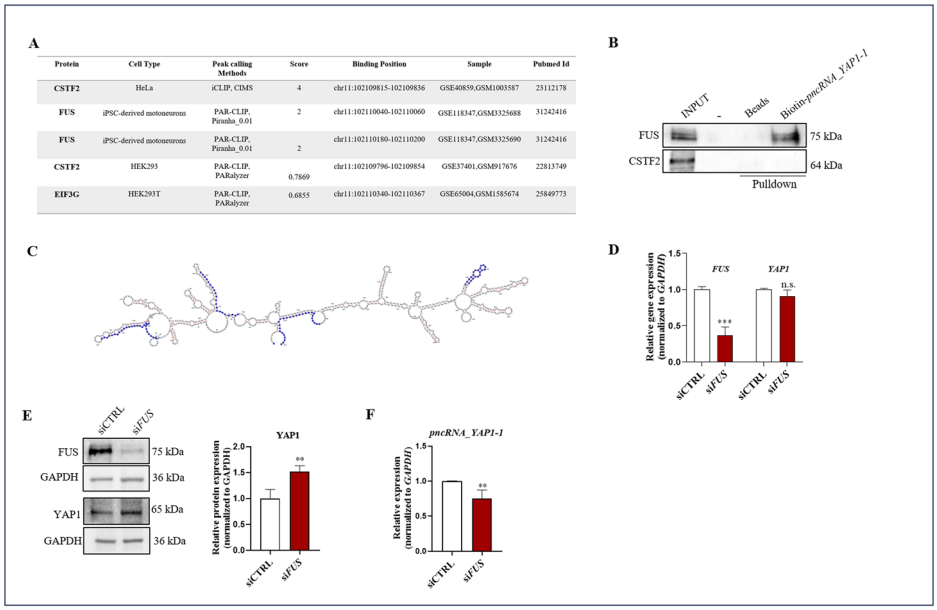

Fig. 6 FUS binds *pncRNA_YAP1-1* and influences YAP1 protein expression. **A** Clip-seq data, obtained from *annolnc* tool (https://annolnc.gao-lab.org/). **B** SK-N-MC extracts were used in RNA pulldown experiments with biotinylated *pncRNA_YAP1-1*, and western blot analysis was performed. **C** Schematic representation of *pncRNA_YAP1-1* obtained by *annolnc* tool (https://annolnc.gao-lab.org/). Putative FUS binding sites are reported in blue. SK-N-MC cells were transfected with a control siRNA (siCTRL) or a siRNA specific for *FUS* (si*FUS*), and *FUS* and *YAP1* expression was analysed using RT-qPCR (**D**) and WB analysis (**E**). **F** SK-N-MC cells were transfected as in **D**, and *pncRNA_YAP1-1* expression was analysed using RT-qPCR. Histograms represent the mean ± SD of three independent experiments, considering the siCTRL as 1. Statistical analyses were performed using Student's *t*-test, *p*-values: $*p \leq 0.05$; $**p \leq 0.01$; $***p \leq 0.001$; $****p \leq 0.0001$

in sarcoma (FUS) [56] (Fig. 6A). To confirm these interactions in ES cells, we performed streptavidin-pulldown assay using biotin-labelled *pncRNA_YAP1-1* as a bait and ES cellular extracts. Western blot analysis of retained RBPs revealed that FUS associates with *pncRNA_YAP1-1* in vitro, whereas CSTF2 was not associated with the *pncRNA_YAP1-1* in our experimental conditions (Fig. 6B). Putative FUS binding sites on *pncRNA_YAP1-1* sequence are shown in Fig. 6C and Supplementary Fig. 5A.

To explore whether FUS is involved in the *pncRNA_YAP1-1*-mediated regulation of YAP1 protein expression, we performed *FUS* knockdown in ES cells. Downregulation of *FUS* did not affect *YAP1* RNA level (Fig. 6D, Supplementary Fig. 5B) but led to upregulation of YAP1 protein, as shown by western blot analysis after *FUS* silencing (Fig. 6E, Supplementary Fig. 5C). Importantly, the *pncRNA_YAP1-1* expression was reduced by *FUS* depletion, both in SK-N-MC and TC-71 cells (Fig. 6F, Supplementary Fig. 5D). Altogether, these data indicate that FUS binds and stabilizes *pncRNA_YAP1-1*, thus impacting YAP1 protein expression.

FUS/*pncRNA_YAP1-1* complex affects YAP1/TEAD interaction

Several reports support the involvement of RBPs in the control of lncRNA subcellular localization [57, 58]. To further explore the possible mechanism of *pncRNA_YAP1-1* regulation, we performed nuclear-cytosolic fractionation to determine whether *FUS* silencing affected *pncRNA_YAP1-1* localization, but we did not observe any change (Fig. 7A, Supplementary Fig. 5E), although we cannot exclude that some transitions in the *pncRNA_YAP1-1* localization occur in sub-nuclear domains. Since YAP1 protein

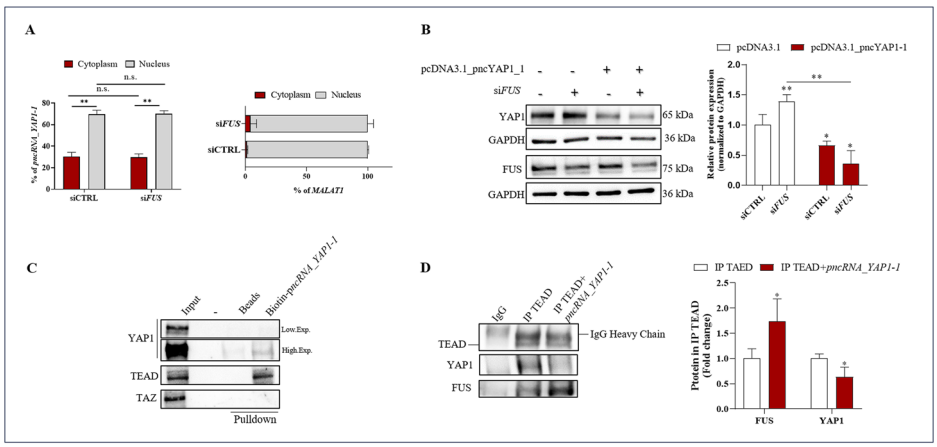

Fig. 7 FUS/*pncRNA_YAP1-1* control YAP1 turnover. **A** SK-N-MC cells were transfected with control siRNA (siCTRL) or siRNA specific for *FUS* (si*FUS*); cytosolic and nuclear RNA was extracted and analysed by RT-qPCR. *MALAT1* was used as nuclear marker. Values are the mean ± SD of three independent experiments, expressed as % of total RNA. **B** SK-N-MC cells were transfected with control siRNA or siRNA specific for FUS (siFUS), as in A, together with pcDNA3.1 or pcDNA3.1_pncRNA_YAP1-1 plasmid. Western blot analysis was performed to monitor YAP1 and FUS expression, GAPDH was used as loading control. *FUS((siFUS)*. Histograms represent the mean ± SD of three independent experiments, considering the siCTRL pcDNA3.1 as 1. Statistical analyses were performed using Student's *t*-test, *p*-values: *, $p \leq 0.05$; **, $p \leq 0.01$. **C** SK-N-MC extracts were used in RNA pulldown experiments with biotinylated *pncRNA_YAP1-1* as bait, and western blot analysis was performed. **D** SK-N-MC extracts were immunoprecipitated with TEAD antibody (IP TEAD) or anti-IgG mouse Abs (IgG), in the presence or not of in vitro-transcribed *pncRNA_YAP1-1*. IP was subjected to WB. Statistical analyses were performed using Student's *t*-test, *p*-value: *$p \leq 0.05$

abundance increased after *FUS* silencing, we hypothesized that *pncRNA_YAP1-1* and FUS are involved in the control of YAP1 turnover in ES cells.

To deeper elucidate this aspect, we analysed YAP1 protein level after *FUS* silencing in condition of *pncRNA_YAP1-1* overexpression. We found that the increase of YAP1 induced by *FUS* silencing was reduced after *pncRNA_YAP1-1* overexpression (Fig. 7B). Taken together, these results indicate that *pncRNA_YAP1-1* is required for the control of YAP1 turnover in ES cells. Downregulation of *FUS* promotes changes in YAP1 basal turnover by affecting *pncRNA_YAP1-1* levels. Since FUS interacted with *pncRNA_YAP1-1* in the nucleus (Fig. 6B), but not with YAP1 (Supplementary Fig. 5F), we asked whether *pncRNA_YAP1-1* itself could interact with YAP1, or with its partners TAZ or *TEA Domain Transcription Factor* (TEAD). RNA pulldown experiments showed that the *pncRNA_YAP1-1* weakly interacted with YAP1, whereas a marked interaction was found with TEAD. No interaction was detected with TAZ (Fig. 7C). Moreover, immunoprecipitation experiments showed that *pncRNA_YAP1-1* overexpression was sufficient to impair TEAD-YAP1 interaction, whilst increasing the interaction of TEAD with FUS (Fig. 7D).

Collectively, these data indicate that the stabilization of *pncRNA_YAP1-1* by FUS binding inhibits the formation of TEAD/YAP1 complex, thus influencing the amount of free YAP1 protein and its consequent degradation.

Changes in the endogenous level of *pncRNA_YAP1-1* affect YAP1 protein expression

It is widely accepted that altered lncRNA expression can impact tumour cell development and anti-tumour drug response [9]. Here we found that modulation of *pncRNA_YAP1-1* expression affects YAP1 protein level. Thus, we tested whether other stimuli could also induce changes in YAP1 expression by modulating *pncRNA_YAP1-1* level. We first assessed the effects induced by conditions typically known to cause cell growth arrest, such as serum deprivation, RAD-001 treatment, which is a well-known mammalian target of rapamycin complex 1 (mTORC1) inhibitor widely used in cancer therapy, and BEZ-235, which is a dual phosphoinositide 3 kinase (PI3K) and mTOR inhibitor. We found that serum deprivation enhanced *pncRNA_YAP1-1* expression, as well as treatment with RAD-001, BEZ-235 and etoposide, commonly used as anticancer drugs (Fig. 8A). In all these conditions, *YAP1* mRNA levels were not affected (Fig. 8B), whereas YAP1 protein levels decreased (Fig. 8C), thus corroborating our hypothetical mechanism (Fig. 8D). Olaparib, which causes apoptosis of cancer cells by blocking the poly (ADP-ribose) polymerase (PARP), did not affect *pncRNA_YAP1-1* expression level nor YAP1 protein expression, thus supporting our model (Fig. 8A–C).

Altogether, these results suggest that modulation of *pncRNA_YAP1-1* levels in response to specific treatments, can influence YAP1 protein expression, thus impacting ES cell growth.

Discussion

The identification of key effectors involved in ES tumour growth and progression is the main challenge in the development of new treatments to integrate with standard therapies [59]. Several well-known signalling pathways contribute to ES oncogenesis. Among them, the Hippo pathway controls several physiological processes within cells, and its

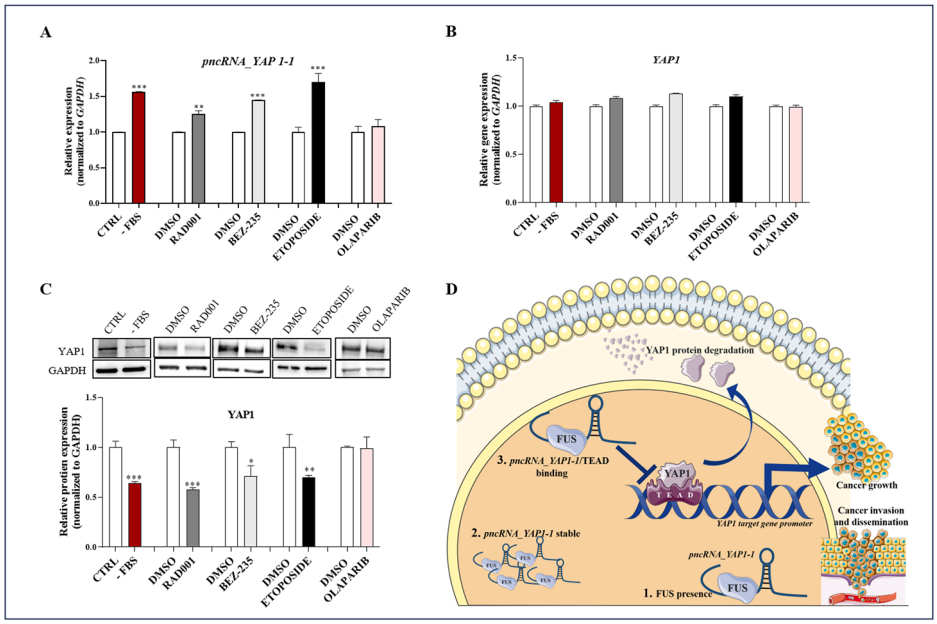

Fig. 8 Induction of *pncRNA_YAP1-1* expression affects YAP1 protein level. **A** and **B** SK-N-MC cells were serum starved (16 h) and treated or not treated with BEZ-235 (300 nM,16 h), RAD001 (25 nM, 16 h), OLAPARIB (300 nM, 24 h) and ETOPOSIDE (5 μM, 24 h) and RNA was extracted and analysed using RT-qPCR. **C** Cells were treated as in **A**, and WB analysis was performed. Histograms represent the mean ± SD of three independent experiments, considering the control sample (CTRL or DMSO) as 1. Statistical analyses were performed using Student's *t*-test, *p*-values: *$p \leq 0.05$; **, $p \leq 0.01$; ***, $p \leq 0.001$; ****, $p \leq 0.0001$. **(D)** Proposed model of YAP1 expression regulation by FUS/*pncRNA_YAP1-1*. Parts of the figure were drawn by using pictures from Servier Medical Art (http://smart.servier.com/), licensed under a Creative Commons Attribution 4.0 Unported License (https://creativecommons.org/licenses/by/4.0/)

oncogenic activation has been linked to ES tumorigenesis [13, 15–19, 52]. The Hippo pathway ultimately converges on the key transducers YAP1 and TAZ, whose aberrant activation has been implicated in various cancers [14]. Given its critical role, YAP/TAZ signalling has been the focus of extensive research efforts, allowing for the development of small-molecule inhibitors to be used in preclinical and clinical studies [13, 14]. The main therapeutic goal of these molecules is the inhibition of the interaction between YAP1 and TEA domain transcription factor 1 (TEAD1), the modulation of the subcellular localization of YAP/TAZ or the modulation of the YAP/TAZ-mediated gene transcription. Along with strategies targeting YAP1 activity, regulating YAP1 protein expression could offer a promising approach. In this context, we identified a mechanism of regulation of YAP1 expression via the DHX9/KDM2B axis in ES [60].

Herein, we have focused on the possibility of downregulating YAP1 expression to counteract ES cell tumorigenicity through pncRNAs. Several studies have highlighted pncRNAs as active players in the process of tumour growth and progression [5, 7]. Moreover, pncRNAs' ability to control gene expression at epigenetic, transcriptional, post-transcriptional, translational and post-translational levels is well documented [9, 12, 46, 47, 57, 61, 62], and a growing number of studies have reported that ncRNAs can directly or indirectly influence YAP/TAZ signalling [20–22, 24, 63–66].

In this study, we have characterized a previously unstudied *YAP1* promoter-associated noncoding RNA, renamed *pncRNA_YAP1-1*, in ES cells. Our findings show that *pncRNA_YAP1-1* can influence YAP1 protein level, resulting in reduced tumour cell growth.

LncRNAs are low abundant RNA species [48]. Consistently, we found low level of *pncRNA_YAP1-1* expression in ES cells, albeit with variations between the different cell lines analysed. Importantly, increased YAP1 and *pncRNA_YAP1-1* levels were detected in ES cells established from patients with metastasis, suggesting that *pncRNA_YAP1-1* could be involved in specific mechanisms responsible in controlling YAP1 expression, also underlying the maintenance of the tumorigenic properties. Indeed, the deregulation of YAP1 protein by *pncRNA_YAP1-1* overexpression contributes to a reduction of YAP1 transcriptional activity, which, in turn, impacts on the cell's ability to proliferate, migrate and invade.

Our findings indicate that *pncRNA_YAP1-1* controls YAP1 protein expression through the interaction with the RBP FUS. The aberrant Hippo pathway cascade converges to YAP/TAZ recruitment and binding to TEAD factors, driving a transcriptional program responsible of the acquisition of cellular changes promoting tumorigenesis [14]. Furthermore, YAP1 binding to its cofactor TEAD is reduced by *pncRNA_YAP1-1*/FUS binding to TEAD itself, causing YAP1 cytoplasmic accumulation and targeting for degradation (Fig. 8D).

Interestingly, *pncRNA_YAP1-1* was significantly up-regulated in response to serum starvation and after PI3K/mTOR inhibition or etoposide treatment. As a result, YAP1 protein levels were reduced in the treated cells, while its mRNA levels remained unaffected. Traditionally, promoter-associated noncoding RNAs act in cis by favouring, or inhibiting, recruitment of transcription factors or chromatin remodelling complexes on the promoter of their host gene [12, 47, 67]. Here, we found that *pncRNA_YAP1-1* destabilizes YAP1-TEAD interaction, thus favouring YAP1 translocation into the cytoplasm and its consequent phosphorylation and degradation. The mechanism relies on FUS binding to the *pncRNA_YAP1-1* and stabilization of the transcript (Fig. 8D). A similar mechanism was described by Li and colleagues for β-catenin, where *pancEts-1* binding to hnRNPK was found to facilitate its physical interaction with β-catenin, thus inhibiting its proteasome-mediated degradation and resulting in transcriptional alteration of target genes associated with neuroblastoma progression [68]. In our study, FUS interaction with the *pncRNA_YAP1-1* stabilizes the transcript, which in turn interferes with the TEAD-YAP1 complex, thus inhibiting their oncogenic transcriptional program. In our study, *pncRNA_YAP1-1* displays an antioncogenic role, promoting YAP1 translocation into the cytoplasm and degradation. Furthermore, we revealed an additional modality of regulation of YAP1 expression in response to different treatments, widely used in cancer therapy, including ES. Hence, we suggest a promising mechanism for therapeutic intervention in ES. Further investigations could clarify whether YAP1 regulation is also present in other tumour types. In addition, changes in *pncRNA_YAP1-1* expression could eventually be leveraged to monitor therapy advancement. The association of *pncRNA_YAP1-1* expression with different tumour stages and therapy response could make it a valuable marker for both carcinogenesis and the overall health status of patients.

Conclusions

Collectively, our findings highlight the role of the *pncRNA_YAP1-1*/FUS axis in regulating YAP1 expression in ES, offering the possibility of an alternative regulatory mechanism, in addition to the canonical YAP1 control. This could potentially be exploited for therapeutic purpose in ES tumours.

Abbreviations

ES	Ewing sarcoma
lncRNAs	Long noncoding RNAs
circRNAs	Circular RNAs
ceRNAs	Competing endogenous RNAs
YAP1	Yes-associated protein 1
TAZ	Transcriptional coactivator with PDZ-binding motif
pncRNAs	Promoter-associated noncoding RNAs
TSS	Transcription start-site
pncRNA_YAP1-1	*YAP1* Promoter-associated ncRNA 1
FBS	Fetal bovine serum
PBS	Phosphate-buffered saline
CHX	Cycloheximide
DMSO	Dimethyl sulfoxide
FISH	Fluorescent in situ hybridization
CLIP-seq	Cross-linking immunoprecipitation sequencing
CTGF	Connective tissue growth factor
CYR61	CYsteine-Rich angiogenic inducer 61
CCND1	Cyclin D1
RBP	RNA binding protein
FUS	Fused in sarcoma
CSTF2	Cleavage stimulation factor subunit 2
TEAD	TEA domain transcription factor
PI3K	Phosphoinositide 3 kinase
mTORC1	Mammalian target of rapamycin complex 1
PARP	Poly (ADP-ribose) polymerase

Supplementary Information

The online version contains supplementary material available at https://doi.org/10.1186/s11658-025-00736-4.

Supplementary Material 1.

Supplementary Material 2.

Acknowledgements

The authors wish to thank Dr Gianmarco Fenili for his support in the bioinformatic analysis of the patients' datasets.

Author contributions

Conceptualization—LC and MPP; methodology—LC; formal analysis—LC; investigation—LC, ADV and VR; writing—original draft preparation—LC; writing—review and editing—LC and MPP; project administration—MPP; funding acquisition—LC and MPP. The authors have read and agreed to the published version of the manuscript.

Funding

This work was supported by grants from the Associazione Italiana Ricerca sul Cancro (AIRC) (IG21877) to MPP, and from the Italian Ministry of Health (SG-2019–12371596) to LC.

Availability of data and materials

All data generated in this study are included in this article and its supplementary files. Original immunoblots are provided in the Supplementary Information File.

Declarations

Ethics approval and consent to participate

Not applicable.

Consent for publication
The article's publication is approved by all authors and tacitly or explicitly by the responsible authorities where the work was carried out.

Competing interests
The authors declare that they have no competing interests.

Received: 14 November 2024 Accepted: 22 April 2025
Published online: 25 May 2025

References

1. Grünewald TGP, Cidre-Aranaz F, Surdez D, Tomazou EM, de Álava E, Kovar H, et al. Ewing sarcoma. Nat Rev Dis Primers. 2018;4(1):5.
2. Gargallo P, Yáñez Y, Juan A, Segura V, Balaguer J, Torres B, et al. Review: Ewing sarcoma predisposition. Pathol Oncol Res. 2020;26(4):2057–66.
3. Ramamurthy A, Connolly EA, Mar J, Lewin J, Bhadri VA, Phillips MB, et al. High-dose chemotherapy for Ewing sarcoma and Rhabdomyosarcoma: a systematic review by the Australia and New Zealand Sarcoma Association Clinical Practice Guidelines Working Party. Cancer Treat Rev. 2024;124: 102694.
4. Riggi N, Suvà ML, Stamenkovic I. Ewing's Sarcoma. N Engl J Med. 2021;384(2):154–64.
5. Barrett C, Budhiraja A, Parashar V, Batish M. The landscape of regulatory noncoding RNAs in Ewing's sarcoma. Biomedicines. 2021;9(8).
6. Statello L, Guo CJ, Chen LL, Huarte M. Gene regulation by long non-coding RNAs and its biological functions. Nat Rev Mol Cell Biol. 2021;22(2):96–118.
7. Aryee DNT, Fock V, Kapoor U, Radic-Sarikas B, Kovar H. Zooming in on long non-coding RNAs in Ewing sarcoma pathogenesis. Cells. 2022;11(8):933.
8. Yang L, Tang L, Min Q, Tian H, Li L, Zhao Y, et al. Emerging role of RNA modification and long noncoding RNA interaction in cancer. Cancer Gene Ther. 2024;31(6):816–30.
9. Bartonicek N, Maag JL, Dinger ME. Long noncoding RNAs in cancer: mechanisms of action and technological advancements. Mol Cancer. 2016;15(1):43.
10. Winkle M, El-Daly SM, Fabbri M, Calin GA. Noncoding RNA therapeutics—Challenges and potential solutions. Nat Rev Drug Discov. 2021;20(8):629–51.
11. Chen B, Dragomir MP, Yang C, Li Q, Horst D, Calin GA. Targeting non-coding RNAs to overcome cancer therapy resistance. Signal Transduct Target Ther. 2022;7(1):121.
12. Mercatelli N, Palombo R, Paronetto MP. Emerging contribution of PancRNAs in cancer. Cancers (Basel). 2020;12(8):2035.
13. Calses PC, Crawford JJ, Lill JR, Dey A. Hippo pathway in cancer: aberrant regulation and therapeutic opportunities. Trends Cancer. 2019;5(5):297–307.
14. Mohajan S, Jaiswal PK, Vatanmakarian M, Yousefi H, Sankaralingam S, Alahari SK, et al. Hippo pathway: regulation, deregulation and potential therapeutic targets in cancer. Cancer Lett. 2021;507:112–23.
15. Han Y. Analysis of the role of the Hippo pathway in cancer. J Transl Med. 2019;17(1):116.
16. Hsu JH, Lawlor ER. BMI-1 suppresses contact inhibition and stabilizes YAP in Ewing sarcoma. Oncogene. 2011;30(17):2077–85.
17. He S, Huang Q, Hu J, Li L, Xiao Y, Yu H, et al. EWS-FLI1-mediated tenascin-C expression promotes tumour progression by targeting MALAT1 through integrin α5β1-mediated YAP activation in Ewing sarcoma. Br J Cancer. 2019;121(11):922–33.
18. Katschnig AM, Kauer MO, Schwentner R, Tomazou EM, Mutz CN, Linder M, et al. EWS-FLI1 perturbs MRTFB/YAP-1/TEAD target gene regulation inhibiting cytoskeletal autoregulatory feedback in Ewing sarcoma. Oncogene. 2017;36(43):5995–6005.
19. Rodríguez-Núñez P, Romero-Pérez L, Amaral AT, Puerto-Camacho P, Jordán C, Marcilla D, et al. Hippo pathway effectors YAP1/TAZ induce an EWS-FLI1-opposing gene signature and associate with disease progression in Ewing sarcoma. J Pathol. 2020;250(4):374–86.
20. Li N, Xie C, Lu N. Crosstalk between Hippo signalling and miRNAs in tumour progression. FEBS J. 2017;284(7):1045–55.
21. Zhang Y, Wang Y, Ji H, Ding J, Wang K. The interplay between noncoding RNA and YAP/TAZ signaling in cancers: molecular functions and mechanisms. J Exp Clin Cancer Res. 2022;41(1):202.
22. Yan H, Li H, Silva MA, Guan Y, Yang L, Zhu L, et al. LncRNA FLVCR1-AS1 mediates miR-513/YAP1 signaling to promote cell progression, migration, invasion and EMT process in ovarian cancer. J Exp Clin Cancer Res. 2019;38(1):356.
23. Di Agostino S, Valenti F, Sacconi A, Fontemaggi G, Pallocca M, Pulito C, et al. Long non-coding MIR205HG depletes Hsa-miR-590-3p leading to unrestrained proliferation in head and neck squamous cell carcinoma. Theranostics. 2018;8(7):1850–68.
24. Wu DM, Wang S, Wen X, Han XR, Wang YJ, Shen M, et al. LncRNA SNHG15 acts as a ceRNA to regulate YAP1-Hippo signaling pathway by sponging miR-200a-3p in papillary thyroid carcinoma. Cell Death Dis. 2018;9(10):947.
25. Ma D, Gao X, Liu Z, Lu X, Ju H, Zhang N. Exosome-transferred long non-coding RNA ASMTL-AS1 contributes to malignant phenotypes in residual hepatocellular carcinoma after insufficient radiofrequency ablation. Cell Prolif. 2020;53(9): e12795.

26. Zhu Y, He D, Bo H, Liu Z, Xiao M, Xiang L, et al. The MRVI1-AS1/ATF3 signaling loop sensitizes nasopharyngeal cancer cells to paclitaxel by regulating the Hippo-TAZ pathway. Oncogene. 2019;38(32):6065–81.
27. Wang J, Huang F, Shi Y, Zhang Q, Xu S, Yao Y, et al. RP11-323N12.5 promotes the malignancy and immunosuppression of human gastric cancer by increasing YAP1 transcription. Gastric Cancer. 2021;24(1):85–102.
28. Li Z, Wang Y, Hu R, Xu R, Xu W. LncRNA B4GALT1-AS1 recruits HuR to promote osteosarcoma cells stemness and migration via enhancing YAP transcriptional activity. Cell Prolif. 2018;51(6): e12504.
29. Geng Z, Wang W, Chen H, Mao J, Li Z, Zhou J. Circ_0001667 promotes breast cancer cell proliferation and survival via Hippo signal pathway by regulating TAZ. Cell Biosci. 2019;9:104.
30. Shi P, Li Y, Guo Q. Circular RNA circPIP5K1A contributes to cancer stemness of osteosarcoma by miR-515-5p/YAP axis. J Transl Med. 2021;19(1):464.
31. Wang X, Chen Y, Liu W, Liu T, Sun D. Hsa_circ_0128846 promotes tumorigenesis of colorectal cancer by sponging hsa-miR-1184 and releasing AJUBA and inactivating Hippo/YAP signalling. J Cell Mol Med. 2020;24(17):9908–24.
32. Zhang X, Xu Y, Qian Z, Zheng W, Wu Q, Chen Y, et al. circRNA_104075 stimulates YAP-dependent tumorigenesis through the regulation of HNF4a and may serve as a diagnostic marker in hepatocellular carcinoma. Cell Death Dis. 2018;9(11):1091.
33. Choe MH, Yoon Y, Kim J, Hwang SG, Han YH, Kim JS. miR-550a-3-5p acts as a tumor suppressor and reverses BRAF inhibitor resistance through the direct targeting of YAP. Cell Death Dis. 2018;9(6):640.
34. Zhao L, Han S, Hou J, Shi W, Zhao Y, Chen Y. The local anesthetic ropivacaine suppresses progression of breast cancer by regulating miR-27b-3p/YAP axis. Aging (Albany NY). 2021;13(12):16341–52.
35. Jin D, Guo J, Wu Y, Chen W, Du J, Yang L, et al. Metformin-repressed miR-381-YAP-snail axis activity disrupts NSCLC growth and metastasis. J Exp Clin Cancer Res. 2020;39(1):6.
36. Chen R, Qian Z, Xu X, Zhang C, Niu Y, Wang Z, et al. Exosomes-transmitted miR-7 reverses gefitinib resistance by targeting YAP in non-small-cell lung cancer. Pharmacol Res. 2021;165: 105442.
37. Sun M, Song H, Wang S, Zhang C, Zheng L, Chen F, et al. Integrated analysis identifies microRNA-195 as a suppressor of Hippo-YAP pathway in colorectal cancer. J Hematol Oncol. 2017;10(1):79.
38. Xu X, Chen X, Xu M, Liu X, Pan B, Qin J, et al. miR-375-3p suppresses tumorigenesis and partially reverses chemoresistance by targeting YAP1 and SP1 in colorectal cancer cells. Aging (Albany NY). 2019;11(18):7357–85.
39. Selth LA, Das R, Townley SL, Coutinho I, Hanson AR, Centenera MM, et al. A ZEB1-miR-375-YAP1 pathway regulates epithelial plasticity in prostate cancer. Oncogene. 2017;36(1):24–34.
40. Kang W, Tong JH, Lung RW, Dong Y, Zhao J, Liang Q, et al. Targeting of YAP1 by microRNA-15a and microRNA-16-1 exerts tumor suppressor function in gastric adenocarcinoma. Mol Cancer. 2015;14:52.
41. Guo Y, Cui J, Ji Z, Cheng C, Zhang K, Zhang C, et al. miR-302/367/LATS2/YAP pathway is essential for prostate tumor-propagating cells and promotes the development of castration resistance. Oncogene. 2017;36(45):6336–47.
42. Muñoz-Galván S, Felipe-Abrio B, Verdugo-Sivianes EM, Perez M, Jiménez-García MP, Suarez-Martinez E, et al. Down-regulation of MYPT1 increases tumor resistance in ovarian cancer by targeting the Hippo pathway and increasing the stemness. Mol Cancer. 2020;19(1):7.
43. Chen X, Wang AL, Liu YY, Zhao CX, Zhou X, Liu HL, et al. MiR-429 involves in the pathogenesis of colorectal cancer via directly targeting LATS2. Oxid Med Cell Longev. 2020;2020:5316276.
44. Sun Z, Zhang Q, Yuan W, Li X, Chen C, Guo Y, et al. MiR-103a-3p promotes tumour glycolysis in colorectal cancer via hippo/YAP1/HIF1A axis. J Exp Clin Cancer Res. 2020;39(1):250.
45. Lin CW, Chang YL, Chang YC, Lin JC, Chen CC, Pan SH, et al. MicroRNA-135b promotes lung cancer metastasis by regulating multiple targets in the Hippo pathway and LZTS1. Nat Commun. 2013;4:1877.
46. Palombo R, Frisone P, Fidaleo M, Mercatelli N, Sette C, Paronetto MP. The promoter-associated noncoding RNA. Cancer Res. 2019;79(14):3570–82.
47. Chellini L, Frezza V, Paronetto MP. Dissecting the transcriptional regulatory networks of promoter-associated non-coding RNAs in development and cancer. J Exp Clin Cancer Res. 2020;39(1):51.
48. Mattick JS. A Kuhnian revolution in molecular biology: most genes in complex organisms express regulatory RNAs. BioEssays. 2023;45(9): e2300080.
49. Shibata M, Ham K, Hoque MO. A time for YAP1: tumorigenesis, immunosuppression and targeted therapy. Int J Cancer. 2018;143(9):2133–44.
50. Paronetto MP, Bernardis I, Volpe E, Bechara E, Sebestyén E, Eyras E, et al. Regulation of FAS exon definition and apoptosis by the Ewing sarcoma protein. Cell Rep. 2014;7(4):1211–26.
51. Palombo R, Verdile V, Paronetto MP. Poison-exon inclusion in DHX9 reduces its expression and sensitizes Ewing sarcoma cells to chemotherapeutic treatment. Cells. 2020;9(2):328.
52. Bierbaumer L, Katschnig AM, Radic-Sarikas B, Kauer MO, Petro JA, Högler S, et al. YAP/TAZ inhibition reduces metastatic potential of Ewing sarcoma cells. Oncogenesis. 2021;10(1):2.
53. Mancarella C, Caldoni G, Ribolsi I, Parra A, Manara MC, Mercurio AM, et al. Insulin-like growth factor 2 mRNA-binding protein 3 modulates aggressiveness of Ewing sarcoma by regulating the CD164-CXCR4 axis. Front Oncol. 2020;10:994.
54. Zhao B, Wei X, Li W, Udan RS, Yang Q, Kim J, et al. Inactivation of YAP oncoprotein by the Hippo pathway is involved in cell contact inhibition and tissue growth control. Genes Dev. 2007;21(21):2747–61.
55. Yao C, Biesinger J, Wan J, Weng L, Xing Y, Xie X, et al. Transcriptome-wide analyses of CstF64-RNA interactions in global regulation of mRNA alternative polyadenylation. Proc Natl Acad Sci USA. 2012;109(46):18773–8.
56. De Santis R, Alfano V, de Turris V, Colantoni A, Santini L, Garone MG, et al. Mutant FUS and ELAVL4 (HuD) aberrant crosstalk in amyotrophic lateral sclerosis. Cell Rep. 2019;27(13):3818-31.e5.
57. Bridges MC, Daulagala AC, Kourtidis A. LNCcation: lncRNA localization and function. J Cell Biol. 2021;220(2).

58. Yao ZT, Yang YM, Sun MM, He Y, Liao L, Chen KS, et al. New insights into the interplay between long non-coding RNAs and RNA-binding proteins in cancer. Cancer Commun (Lond). 2022;42(2):117–40.
59. Grünewald TG, Alonso M, Avnet S, Banito A, Burdach S, Cidre-Aranaz F, et al. Sarcoma treatment in the era of molecular medicine. EMBO Mol Med. 2020;12(11): e11131.
60. Chellini L, Scarfò M, Bonvissuto D, Sette C, Paronetto MP. The DNA/RNA helicase DHX9 orchestrates the KDM2B-mediated transcriptional regulation of YAP1 in Ewing sarcoma. Oncogene. 2024;43(4):225–34.
61. Palombo R, Paronetto MP. *pncCCND1_B* engages an inhibitory protein network to downregulate CCND1 expression upon DNA damage. Cancers (Basel). 2022;14(6):1537.
62. Wang X, Arai S, Song X, Reichart D, Du K, Pascual G, et al. Induced ncRNAs allosterically modify RNA-binding proteins in cis to inhibit transcription. Nature. 2008;454(7200):126–30.
63. Liu G, Huang K, Jie Z, Wu Y, Chen J, Chen Z, et al. CircFAT1 sponges miR-375 to promote the expression of Yes-associated protein 1 in osteosarcoma cells. Mol Cancer. 2018;17(1):170.
64. Mou K, Liu B, Ding M, Mu X, Han D, Zhou Y, et al. lncRNA-ATB functions as a competing endogenous RNA to promote YAP1 by sponging miR-590-5p in malignant melanoma. Int J Oncol. 2018;53(3):1094–104.
65. Jin Z, Chen B. LncRNA ZEB1-AS1 regulates colorectal cancer cells by MiR-205/YAP1 axis. Open Med (Wars). 2020;15:175–84.
66. Wang W, Li Y, Zhi S, Li J, Miao J, Ding Z, et al. LncRNA-ROR/microRNA-185-3p/YAP1 axis exerts function in biological characteristics of osteosarcoma cells. Genomics. 2021;113(1 Pt 2):450–61.
67. Costa FF. Non-coding RNAs: meet thy masters. BioEssays. 2010;32(7):599–608.
68. Li D, Wang X, Mei H, Fang E, Ye L, Song H, et al. Long noncoding RNA pancEts-1 promotes neuroblastoma progression through hnRNPK-mediated β-catenin stabilization. Cancer Res. 2018;78(5):1169–83.

Publisher's Note